

The Pech-de-l'Azé I Neandertal child: ESR, uranium-series, and AMS ^{14}C dating of its MTA type B context

M. Soressi ^{a,*}, H.L. Jones ^b, W.J. Rink ^c, B. Maureille ^d, A.-m. Tillier ^d

^a Max Planck Institute for Evolutionary Anthropology, Dept. of Human Evolution, Deutscher Platz 6, D-04103 Leipzig, Germany

^b University of Wyoming, Dept. of Geology & Geophysics, Dept. 3006, 1000 E. University Ave. Laramie, WY 82071, USA

^c School of Geography and Earth Sciences, McMaster University, 1280 Main St. W., Hamilton, Ontario L8S 4K1, Canada

^d LAPP, UMR 5199-PACEA, Université Bordeaux I, av. des Facultés, F-33405 Talence cedex, France

Received 26 December 2005; accepted 30 November 2006

Abstract

The Pech-de-l'Azé I skull and mandible are included in the juvenile Neandertal remains from Europe. However, some preserved features in the cranial skeleton seem to distinguish the specimen from other Neandertal children. Unfortunately, the stratigraphic position and dating of this child has never been clear. Our recent work on unpublished archives show that the Pech-de-l'Azé I Neandertal child was discovered at the bottom of layer 6, attributed to the Mousterian of Acheulean tradition type B. These skull and mandible are the first diagnostic human remains (aside from an isolated tooth) attributed to the Mousterian of Acheulean tradition (MTA) type B. Consequently, we confirm that Neandertals were the makers of this Mousterian industry, which is characterized by unusual high frequencies of Upper Paleolithic type tools, elongated blanks and blades. We were able to date the context of the hominid remains by dating layer 6 and the layers above and beneath it using ESR, coupled ESR/ $^{230}\text{Th}/^{234}\text{U}$ (coupled ESR/U-series), and AMS ^{14}C . Coupled ESR/U-series results on 16 mammalian teeth constrain the age of the uppermost layer 7 to 41–58 ka, and layer 6 to 37–51 ka. The wide spread in each age estimate results mainly from uncertainties in the gamma-dose rate. These ages are concordant with AMS ^{14}C ages of two bones coming from the top of layer 6, which provide dates of about 41.7–43.6 ka cal BP. A combination of stratigraphic arguments and dating results for layers 6 and 7 show that the Neandertal child cannot be older than 51 ka or younger than 41 ka. The lowermost layer 4 is shown to be older than 43 ka by the principle of superposition and ESR dating in the immediately overlying layer 5. This study shows that the MTA type B had been manufactured by Neandertals before the arrival of anatomically modern humans in the local region. Additionally, by providing a firm chronological framework for the specific morphometric features of Pech-de-l'Azé I Neandertal child, this study is a new step toward the understanding of temporal and spatial changes in the ontogenesis of Neandertals in south-western Europe during oxygen isotope stages 5–3.

Résumé

Le crâne et la mandibule du Pech-de-l'Azé I sont classiquement inclus dans l'échantillon des restes juvéniles néandertaliens européens. Cependant ils présentent quelques traits anatomiques qui les distinguent au sein de cet échantillon. Un cadre chronologique précis est alors indispensable pour définir si cette variabilité est d'ordre temporel. Jusqu'à récemment, leur position stratigraphique n'avait pas été clairement établie et par conséquent leur contexte n'avait jamais pu être daté précisément. L'étude des archives inédites de Peyrony, de Bordes et d'autres, ainsi que l'analyse des produits de la dernière fouille extensive menée sur le site par Bordes en 1970 et 1971, permettent de montrer que l'enfant du Pech-de-l'Azé I provient de la base du niveau 6, attribué au Moustérien de tradition acheuléenne de type B. Il s'agit de la première tête osseuse néandertalienne que l'on peut associer à cette industrie originale par son fort taux d'outils type Paléolithique supérieur, de lames et d'éclats

* Corresponding author. Tel.: +49 341 35 50 371; fax: +49 341 35 50 399.

E-mail addresses: soressi@eva.mpg.de (M. Soressi), hazellee@uwyo.edu (H.L. Jones), rinkwj@mcmaster.ca (W.J. Rink), b.maureille@anthropologie.u-bordeaux1.fr (B. Maureille), am.tillier@anthropologie.u-bordeaux1.fr (A.-m. Tillier).

allongés. Les Néandertaliens doivent donc être considérés comme les auteurs du MTA de type B. Nous avons utilisé différentes méthodes (RPE, séries de l'Uranium couplées à la RPE et C14 par accélérateur) pour dater le niveau qui a livré les restes néandertaliens et les niveaux sous-jacents et sus-jacents.

Seize dents de grands mammifères ont été datées par RPE. Douze de ces dents ont été choisies dans l'échantillon fouillé par Bordes dans les années 70: elles étaient encore recouvertes du sédiment originel ce qui permet une mesure RPE de bonne qualité. Quatre dents supplémentaires ont été prélevées sur le témoin actuel lors des mesures de dosimétrie. Deux de ces dents ont été datées par les séries de l'Uranium. Les isotopes du carbone ont été mesurés sur deux fragments de diaphyse non brûlés.

Les mesures des séries de l'Uranium couplées à l'ESR montrent que l'âge du niveau 7, le dernier niveau de la séquence, se situe entre 41 et 58 ka, et que l'âge du niveau 6 se situe entre 37 et 51 ka. La large distribution de chaque âge est le résultat d'incertitudes dans le taux de la dose gamma. Ces âges sont concordants avec les deux mesures C¹⁴ AMS qui donnent un âge moyen pour le sommet du niveau 6 d'environ 38 ka, ce qui pourrait correspondre à un âge calendaire calibré entre 41.7 et 43.6 ka cal BP. L'ensemble des arguments stratigraphiques et des résultats des datations radiométriques pour les niveaux 6 et 7 montrent que l'enfant néandertalien ne peut pas être plus vieux que 51 ka, ni plus jeune que 41 ka. Le niveau 4, à la base de la séquence stratigraphique, n'a pas pu être daté directement mais sa position stratigraphique sous le niveau 5 daté par ESR montre que ce niveau 4 est plus ancien que 43 ka. Cette étude montre que le MTA de type B a été produit par les Néandertaliens, avant l'arrivée des Hommes anatomiquement modernes, dans cette région de l'Europe de l'Ouest. En outre, ces nouvelles données précisent le contexte chronologique du fossile de Pech-de-l'Azé I et devraient contribuer à une meilleure compréhension des caractéristiques morphométriques présentées par cet enfant en terme d'évolution régionale. Au fur et à mesure de la datation radiométrique des autres spécimens, la question de changements temporels et spatiaux dans l'ontogenèse des Néandertaliens au cours des stades isotopiques 5 à 3 pourra être précisée.

© 2006 Elsevier Ltd. All rights reserved.

Keywords: Neandertal; Pech-de-l'Azé I; Radiometric dating; ESR; U-series; AMS ¹⁴C; Mousterian of Acheulean tradition type B

Introduction

When scholars attempt to address the question of evolution in the Neandertal lineage, they traditionally compare a “pre-Neandertal” sample [European fossils associated with oxygen isotope stages (OIS) 9–7/6] to a sample of “classical Neandertals” (European fossils related to OIS 5–3). Such an approach obscures the classical and late Neandertal diversity, and the occurrence of individual and/or chronological variation within this latter sample cannot be disregarded, as recently shown by the demonstration of mtDNA diversity of OIS 5–3 Neandertals (Orlando et al., 2006).

The Pech-de-l'Azé I Neandertal child (Fig. 1) has been studied by various scholars, and all of them have stressed that, in addition to a suite of features that are found in archaic members of *Homo sapiens*, including Neandertals, this specimen exhibits some morphological peculiarities (Patte, 1957; Ferembach, 1969; Ferembach et al., 1970; Tillier, 1996). Tillier (1996) presented evidence of ontogenetic variation between Pech-de-l'Azé I and other children of the same age class

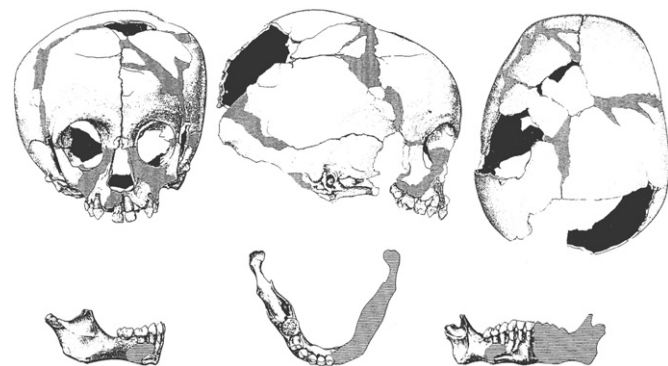


Fig. 1. Pech-de-l'Azé I juvenile Neandertal remains (after Ferembach et al., 1970). Not to scale.

from the Dordogne region, such as the Roc de Marsal 1 individual. For example, the symphyseal region of the Pech de l'Azé I mandible is more gracile (i.e., more modern) than that of Roc de Marsal 1. However, a clear chronological framework for these specimens is required to understand the origin of this morphological variation.

Pech-de-l'Azé I is located northwest of the small village of Carsac within the Dordogne region in southwestern France (approximately 44°50'N, 1°14'E). It is part of a complex of four separate Pleistocene rock-shelters: Pech-de-l'Azé I through Pech-de-l'Azé IV (Bordes and Bourgon, 1950, 1951; Bordes, 1954, 1955, 1975; McPherron and Dibble, 2000; Soressi et al., 2002). In 1909, at the entrance of the Pech-de-l'Azé I cave, Capitan and Peyrony (1909, 1910) recovered the cranium and mandible of a Neandertal child in a layer attributed to the “Upper Mousterian” at the time of the discovery and subsequently attributed to the Mousterian of Acheulean tradition (MTA) (Peyrony, 1920). The lack of precision in the original publication by Capitan and Peyrony prompted Bordes to contest this attribution in the 1970s (Bordes, 1972: 92). The context of the juvenile skull has since remained unclear.

Recent work on both the unpublished notes from Peyrony, Bordes, and others and on the analyses of the unpublished products of the last excavation at Pech I in the 1970s has allowed us to precisely define the original context of the Pech-de-l'Azé I Neandertal child and select appropriate layers to date using ESR, uranium-series, and AMS ¹⁴C.

The context of the Pech-de-l'Azé I Neandertal remains

Capitan and Peyrony (1909) discovered the Pech-de-l'Azé I Neandertal skull while excavating a 1-m-wide trench under the drip line at the entrance of the cave (Fig. 2). The human fossil was discovered near the northwest-facing cliff (Peyrony's oral

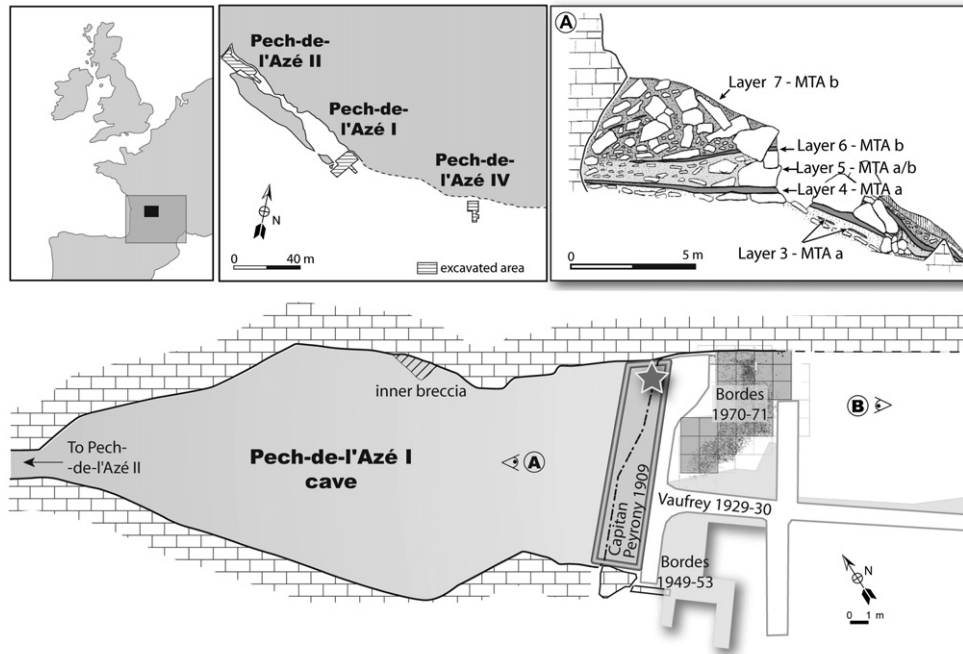


Fig. 2. Location of Pech-de-l'Azé I, II, and IV (redrawn from Bordes, 1972: 7; McPherron and Dibble, 2000), stratigraphy of Pech-de-l'Azé I (after Bordes, 1954), and plan view of the successive excavations at Pech-de-l'Azé I. Discovery location of the Neandertal child is indicated by a star.

communication to Bordes in 1950, published in Bordes, 1984: 147): it was “10 cm deep within the layer,” which was “about 1 m thick ... [and] covered with 3 meters of big limestone blocks and éboulis.” Around the skull, there was an “abundance of broken bones, and the teeth of bovinds, red deer, horses, goats and reindeers,” as well as “many flints: points and knives-scrapers well worked on one face only, and of Upper Mousterian type.... Below the skull, the Mousterian layer contained fine axes of the Saint-Acheul type” (Capitan and Peyrony, 1909: 402). Peyrony (1920) changed the name of the “Upper Mousterian type” layer to “Mousterian of Acheulean tradition” (MTA). Vaufrey (1933) and Bordes (1954, 1955, 1972), who excavated the site after Peyrony, also attributed the entire sequence to the MTA, characterized by bifaces, backed knives and Upper Paleolithic type tools. Bordes used the site as a reference to define two new subspecies within the MTA: MTA type A, after Pech I bottom layer—layer 4—and the MTA type B after the upper layers—layers 5–7—with subtype A characterized by many more bifaces than subtype B (Bordes and Bourgon, 1951; Bordes, 1954, 1955).

Nonetheless, Bordes contested the attribution of the Neandertal remains to the MTA in the early 1970s. He claimed that the Pech-de-l'Azé I human fossil came either from a Denticulate or a Typical Mousterian layer or from a Quina Mousterian layer. In both cases, these layers would not have been recognized by Peyrony and Capitan during their excavation (Bordes, 1972: 23–27, 92).

The putative Denticulate/Typical Mousterian breccia

Bordes grounded his argument about the Denticulate or Typical Mousterian in his recognition of a few stone tools in

a breccia inside the cave, which he attributed to these Mousterian variants (conflicting with Vaufrey’s attribution of this breccia in the 1930s to the MTA). The U/Th dating of the inside breccia by Schwarcz and Blackwell (1983) neither contradicted nor supported Bordes’s hypotheses. What had been dated was the pure calcite flowstone at the bottom of the breccia, underlying the artifacts. However, our recent work at the site shows that:

- 1) The inner cave breccia is at the same elevation as the MTA type B layers from outside of the cave (Fig. 3).
- 2) It is possible to follow the remains of the second (from the top) MTA type B layer (layer 6 in Bordes’s terminology)—still adhering to the cliff—from the existing sections, through the area excavated in the 1970s, to the inside cave breccia. These two are then in direct continuity across the site.

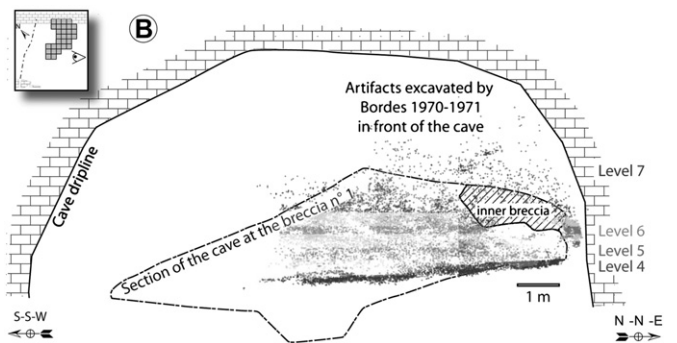


Fig. 3. Cross-sectional view of the artifacts excavated by Bordes in the 1970s, compared with the position of the inner breccia, looking northwest from outside toward inside the cave (see Fig. 2 for direction of the view).

- 3) Calcite flowstone, which forms the breccia, is common in karst environments and is related to local water dripping. Consequently, this layer could have been locally brecciated while laterally lacking calcite cement. This fact was recognized by Bordes himself in the 1970s when he excavated the nearby area excavated by Capitan and Peyrony. He recorded the brecciated parts of layer 6 within the same layer 6 as the nearby nonbrecciated area. Unfortunately, this was done after the publication of his Denticulate/Typical Mousterian hypothesis.
- 4) The MTA type B layers 6 and 7 are very rich in denticulates (more than 50% of the retouched tools are notches and denticulate; see Bordes, 1955), and the small sample collected within the breccia by Bordes may be biased against backed knives, which differentiate the MTA type B from the Denticulate Mousterian, as bifaces are always much rarer than backed knives within the MTA type B (see Bordes, 1972: 54; for example, in Pech I layers 6 and 7, there are 4 and 8 bifaces, 61 and 51 backed knives, and 214 and 217 denticulates and notches, respectively; see details in Soressi, 2002: 162, 169).

The supposed interstratified Quina Mousterian

Bordes highlighted the fact that reindeer are generally characteristic of Quina Mousterian context and that it is possible that what was called an “Upper Mousterian” by Peyrony in 1909 was a Quina Mousterian. However, Mellars (1996: 183–190, 325–331) and others have shown that no Quina Mousterian has ever been found interstratified within MTA layers. Additionally, reindeer are rare at Pech I—they represent 1.4% of the number of identified specimens (NISP) in layer 6 (Rendu, personal communication) and 3.9% of the NISP in layer 4 (Armand et al., 2001). In fact, Peyrony cited the different species in numerical order, as recognized in layer 6, from the most-represented species (bos/bison and red deer) to the least represented (horses, goats, and reindeer) (Rendu, personal communication). Moreover, with a careful and exhaustive reading of the publications by Peyrony and others, published between 1909 and 1950, it is possible to demonstrate that what was called an “Upper Mousterian” with “points and knives-scrapers well worked on one face only” by Peyrony in 1909 was not a Quina Mousterian, but an MTA (Maureille and Soressi, 2000). Finally, two unpublished letters written by Capitan and Peyrony at the time of the discovery were recently found in the archives of the Musée de l’Homme in Paris. These letters confirm that the human remains were found in a “very late Mousterian,” that is “the industry of the Abri Audit and of the site of Gare de Couze” (for a transcription of the two letters, see Maureille and Soressi, 2000). The sites of Abri Audit and Gare de Couze were later used by Peyrony (1920), along with Pech-de-l’Azé I, to define the MTA in opposition to the Quina Mousterian (and Bordes agreed with this classification; see Bordes, 1961: pl. 36–37; 1953: 462).

It is worth noting that Bordes did publish his arguments about the non-MTA origin of Pech-de-l’Azé I child while he

was, with others (e.g., Vallois, 1958), defending the existence of a “pre-sapiens” lineage (a European ancestral population of Upper Paleolithic *Homo sapiens sapiens*) coexisting with the Neandertal lineage (for a more complete review of this theory, see Hublin, 1988). Within this framework, MTA must have been made by “pre-sapiens,” as MTA was, from a cultural point of view, at the origin of the Châtelperronian, considered, since the 1930s, the first Upper Paleolithic-type industry in the area. It is much easier today to look more objectively at the data, as the pre-sapiens theory has been abandoned for about 20 years (Hublin, 1988).

The actual context of Pech-de-l’Azé I Neandertal child

When mapping the artifacts recovered by Bordes in 1970–1971, and comparing this plot to the elevation data for the layers published by Capitan/Peyrony and Vaufrey, the upper limit of the first (from the top) dense archaeological layer, layer 6, remains at the same elevation across the total 8-m-wide excavated area (Maureille and Soressi, 2000). Fortunately, these layers are relatively horizontal across the entire excavation. Peyrony actually found the Neandertal child 10 cm inside what was later called layer 6. Due to the fact that this layer 6 is always equal to or thicker than 10 cm, and because it is of about the same thickness across the known part of the site, we can assume that the Neandertal child comes from layer 6 or from the interface between layer 6 and layer 5. To be conservative, the possibility that the child could have been buried into layer 6 by people inhabiting the site during the formation of layer 7 should be considered. Regardless, we conclude that the Pech-de-l’Azé I Neandertal child is associated with MTA type B, and cannot be older than the formation of layer 6. These are the first significant diagnostic human remains attributed to the MTA type B [aside from a Neandertal lower first premolar from La Quina bed 6d (Debénath and Jelinek, 1998; Verna, 2006: 436)]. Consequently, we confirm that Neandertals were the makers of this Mousterian industry with unusual high frequency of Upper Paleolithic type tools, elongated blanks and blades (Bordes, 1984: 142–149; Soressi, 2002: 218–238).

Radiometric the dating of Pech-de-l’Azé I upper layers

Accurate dating of the Pech-de-l’Azé I Neandertal child is dependent upon reliable dating of layer 6, as well the underlying and overlying layers 5 and 7, respectively. Burnt stone artifacts are rare at Pech-de-l’Azé I within these layers, whereas teeth of large mammals are relatively common. Therefore, we used electron spin resonance (ESR) dating of tooth enamel coupled with uranium-series dating of the tooth dentine and AMS ¹⁴C dating of unburnt bone to substantiate the chronology at Pech-de-l’Azé I.

Methodology, ESR, and uranium-series sample

Electron spin resonance dating of mammalian tooth enamel has been used at many archaeological sites that are beyond the

range of radiocarbon dating (e.g., reviews by Rink, 1997, 2000). Mammalian tooth enamel is composed of the mineral hydroxyapatite, which exhibits an ESR signal produced from the passage effects of radiation during the tooth's burial and has a theoretical lifetime of 10^9 years (Schwarcz, 1985). Alpha (α), beta (β), gamma (γ), and cosmic (χ) radiation dose rates must be evaluated to determine ESR-model ages. The outer and inner ~ 40 – 50 μm of enamel of each specimen was stripped with a hand-held diamond wheel saw to remove enamel exposed to alpha radiation. Neutron activation analysis (NAA) of the thorium and potassium and delayed neutron counting to determine uranium in the sample's surrounding sediment provided the environmental beta-dose rates the samples received during burial. Gamma-dose rates were measured in situ within the excavation profile using a Nutmaq-Harwell Gamma Spectrometer. Cosmic-dose rates were determined using the estimated overburden depth of the samples plus a correction for the estimated height of the cliff backing one side of the site (a major form of shielding against cosmic-ray irradiation at the site). All of these sources of dose accrue a stored dose in the enamel, which is evaluated in the ESR experiment.

The ratio of accrued dose (assessed as the equivalent dose) to the total dose rate yields the ESR-model age. For teeth that have absorbed uranium, two model ages are usually calculated: (1) early uptake (EU) and (2) linear uptake (LU). These differ because the dose rate from uranium is assumed to be different in each model. The EU model assumes that all of the absorbed uranium arrived instantaneously at burial, while the LU model assumes a gradual, constant uptake of uranium throughout the burial history. Grün et al. (1988) and Grün and McDermott (1994) showed that U-series analyses of dental tissues from teeth that had already been studied with ESR could provide a way to better constrain the uranium-uptake history in a tooth. Commonly referred to as coupled or combined ESR/U-series dating, this methodology uses relevant isotopic ratios of Th and U from the U-series analysis in combination with the ESR equivalent-dose and dose-rate data. Together, these yield an age that is consistent with all of the dose rates and attributes a specific applicable uptake function characterized by a p-value. A p-value of 0 equates to a constant or linear uranium uptake, while a p-value of -1 represents early uptake; intermediate values represent behaviors between early and linear uptake. Very large values of p ($>>1$) represent uptake occurring late in the burial, called recent or late uptake. The resulting ESR-model ages can then be coupled with a closed-system uranium-series age from the dentine of the corresponding tooth.

Twelve of the sixteen mammalian-tooth samples that were dated by ESR techniques and are reported here were originally excavated during Bordes's 1970–1971 field season. Ten of the teeth are of unspecified cervid affinities, three are unspecified bovid, two are wild goat, and one is from a wild ass (taxonomic determination by D. Armand, personal communication; Table 1). Of the 16 teeth, four were subsampled for a total of 20 ESR ages. The previously excavated tooth samples had remained at the Institut de Préhistoire et de Géologie du Quaternaire at the University of Bordeaux unwashed, unlabeled,

and classified by square rather than by layer. In 1999, the entire excavation collection ($\sim 15,000$ pieces) was curated and entered into a database. Sediments from unwashed tooth samples were collected and analyzed for beta-dose-rate approximations. Two of us (WJR and MS) collected four additional teeth and their surrounding sediment in the exposed profile while conducting gamma-dosimetry measurements. Teeth from the archive were selected for their proximity to the remaining profile for gamma dosimetry and for presence of attached sediment, which is used for beta-dose-rate calculations. Precise locations of the teeth from layers 5–7 were transcribed from Bordes's field notes. Because Pech I is a "lumpy," or a sedimentologically heterogeneous, site (see section drawing in Fig. 4), several gamma-dose rates were measured for each layer and then averaged to compensate for heterogeneity of each layer (Schwarcz, 1994; Brennan et al., 1997; Table 2). A total of eight gamma-radioactivity measurements were taken using a Nutmaq-Harwell Gamma Spectrometer; the locations are listed in Table 2 and shown in Fig. 4. All ESR-dated teeth were originally located within 2–3 m of the in situ gamma dosimetry, with the exception of ESR 12 (Fig. 4A). It should be noted that dosimetry-location selection was directly limited by the position of the relict cross-sectional profile that remains at the site and should be a source of concern and caution when working at a historical excavation site.

Sediment-moisture-content samples were taken from the rear of the horizontal gamma holes (~ 30 cm deep) and ranged from 3 to 10% dry weight. A conservative value of $10 \pm 10\%$ moisture content was assumed for the entire burial history of the samples. For further details of ESR- and U-series-sample preparation and analysis, see Jones et al. (2004). The ESR-model ages (EU and LU) were calculated using ESR-dating software Rosy v.2, which uses "one-group" transport calculations for beta dosimetry (Brennan et al., 1997, 1999). The coupled ESR/U-series ages were calculated using the software DATA-WJR.exe courtesy of R. Grün (Australian National University, Canberra, Australia) and are based on Monte Carlo calculations of the beta-dose rates (Marsh et al., 2002).

ESR/uranium-series results

The uranium concentrations in the enamel samples were very low. Twelve of sixteen samples had uranium concentrations that were below the detectable limit (0.1 ppm) of delayed neutron activation analysis (DNAA), and none of the enamels had uranium concentrations of greater than 0.6 ppm. The uranium concentrations in the dentine samples generally decreased with depth and ranged from ~ 1 to 15 ppm (Table 1). The locations of the external-gamma-dosimetry measurements and resulting average dose rates are given in Table 2 and plotted in Fig. 5. Both the variability of gamma doses as a result of the "lumpiness" (sensu Schwarcz, 1994) of the site and the gamma dosimetry being performed 30 years after the excavation leads to larger uncertainty in the age. An uncertainty of $\pm 20\%$ was applied to the layer-averaged gamma doses. This uncertainty envelops the variation for the layer-averaged

Table 1
Analytical data for teeth from Pech-de-l'Azé I

Mac field #	Taxon	Square	Layer	D _E * (Gy)	U En** (ppm)	U Den** (ppm)	U Sed** (ppm)	Th Sed ³ (ppm)	K Sed ³ (Wt%)	Enamel thickness [§] (μm)	Rem 1 ^{§§} (μm)	Rem 2 ^{§§} (μm)
ESR 0A	Wild goat	F10	7 middle	24.39 ± 0.44	0.21	5.22	1.81	5.17	0.52	881 ± 108	47 ± 24	24 ± 12
ESR 1A	Bovid	F10	7 middle	19.24 ± 1.95	<0.1	6.05	6.05	6.41	0.71	1086 ± 72	52 ± 26	41 ± 21
ESR18A	Cervid	I8	7 base	25.39 ± 1.67	<0.1	5.86	1.79	5.06	0.42	962 ± 88	34 ± 17	52 ± 26
ESR19A	Cervid	I8	7 base	24.92 ± 4.75	<0.1	6.72	1.29	4.51	0.48	879 ± 95	56 ± 28	69 ± 35
ESR20A	Cervid	I8	7 base	20.91 ± 1.35	0.45	8.16	1.34	4.46	0.50	990 ± 122	66 ± 33	37 ± 19
ESR21A	Cervid	I8	7 base	19.84 ± 1.15	<0.1	7.82	1.38	6.28	0.47	1134 ± 185	39 ± 20	99 ± 50
ESR21B	Cervid	I8	7 base	21.02 ± 1.26	<0.1	8.13	1.38	6.28	0.47	1091 ± 67	56 ± 28	57 ± 29
ESR 2A	Bovid	F10	7 base	18.90 ± 2.10	0.59	5.01	2.19	3.10	0.42	839 ± 58	47 ± 24	58 ± 29
ESR 3A	Cervid	F10	7 base	22.12 ± 0.98	0.21	13.78	1.18	3.10	0.43	998 ± 78	90 ± 45	65 ± 33
ESR 3B	Cervid	F10	7 base	21.57 ± 1.26	<0.1	14.04	1.18	3.10	0.43	1041 ± 108	114 ± 57	20 ± 10
ESR 4A	Cervid	F10	7 base	22.08 ± 1.49	<0.1	15.34	1.33	6.20	0.48	874 ± 46	44 ± 22	60 ± 30
ESR 5A	Wild goat	F10	7 base	19.22 ± 1.41	0.46	11.04	1.14	4.84	0.52	660 ± 49	53 ± 27	41 ± 21
ESR 5B	Wild goat	F10	7 base	21.57 ± 3.14	<0.1	10.28	1.14	4.84	0.52	779 ± 96	53 ± 27	35 ± 18
ESR 7A	Cervid	F10	7 base	18.48 ± 1.03	0.50	10.02	1.74	4.99	0.44	1003 ± 70	42 ± 21	33 ± 17
ESR 8A	Wild ass	F10	6	22.94 ± 0.87	<0.1	4.98	1.90	4.65	0.40	1036 ± 102	82 ± 41	41 ± 20
ESR 8B	Wild ass	F10	6	21.65 ± 1.27	0.26	2.99	1.90	4.65	0.40	1013 ± 46	65 ± 33	45 ± 23
ESR 9A	Cervid	F7	6 base	22.32 ± 1.45	0.09	9.44	2.08	5.70	0.50	936 ± 56	32 ± 16	64 ± 32
ESR10A	Cervid	G10	5	20.76 ± 0.68	<0.1	1.58	1.09	5.57	0.56	1071 ± 60	65 ± 33	30 ± 15
ESR12A	Bovid	E13	5	20.01 ± 0.84	<0.1	4.33	1.54	4.09	0.53	1365 ± 65	26 ± 13	98 ± 49
ESR13A	Cervid	G9	5 base	28.67 ± 1.14	<0.1	3.52	1.48	6.49	0.47	884 ± 54	39 ± 20	50 ± 25

* Equivalent dose (D_E) in Grays (Gy).

** Uranium in enamel (En), dentine (Den), and sediment (Sed) is determined by delayed neutron counting in parts per million (ppm) with a detection limit of 0.1 ppm.

³ Thorium (Th) and potassium (K) concentrations in parts per million (ppm) and weight percent (Wt%) were determined by neutron activation analysis. Uncertainty levels were insignificant to calculations of annual doses.

[§] Each sample measured in 40–100 positions using a micrometer indicator with a precision of ±2 μm; the reported uncertainties are ±1σ.

^{§§} Amount of enamel stripped from the external side (Rem 1) and the internal side (Rem 2) to remove damage due to alpha radiation. The uncertainty was estimated to be 50% of the removed portion.

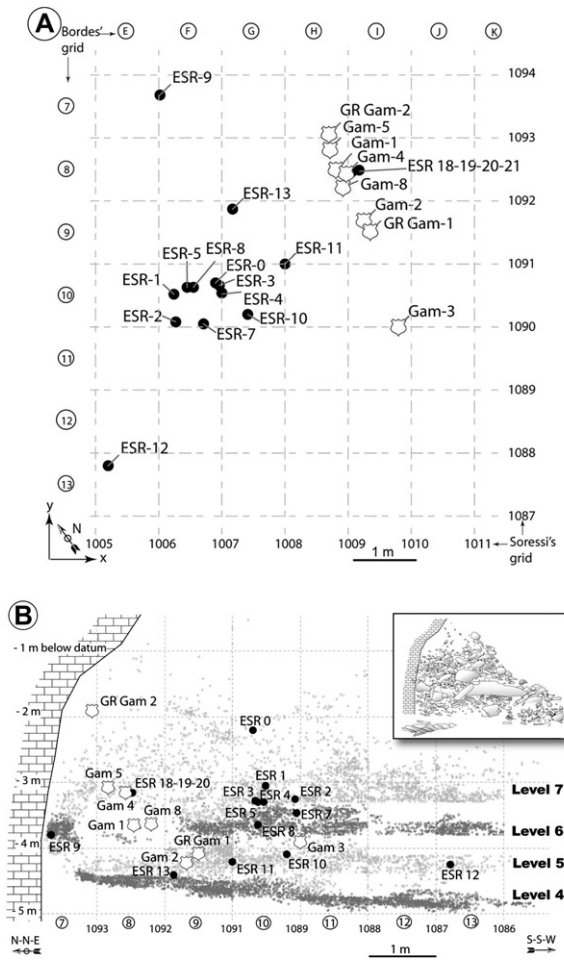


Fig. 4. Location of the dated teeth and the dosimetry measurements: (A) plan view; (B) cross-sectional view looking northeast (inset: schematic drawing of the section without data points).

gamma-dose rates for layers 6 and 7, but not layer 5. It is postulated that the low gamma-dose rate for GAM 3 in layer 5 is due to its proximity to a large limestone block.

All dose rates associated with the ESR-model ages (EU and LU) are tabulated in Table 3. The relatively high U concentrations in the dentine of teeth from layers 6 and 7 required that uranium-series analyses of dentine be performed in order to refine the ESR-model ages using uranium-series analysis (Grün et al., 1988) of some of those teeth. The U-series results are given in Table 4. The closed-system uranium-series ages on each of two dentine samples do not provide the burial age of the tooth containing the dentine because the dentine behaved as an open system (see below), with uranium being absorbed throughout different portions of the burial history and at different rates. The closed-system $^{230}\text{Th}/^{234}\text{U}$ disequilibrium ages (U-series ages) that are reported in Table 4 are provided here only because it is useful to compare them to the ESR-model ages.

The individual ESR-model ages for each sample, mean ESR-model ages for each layer, and two coupled ESR/U-series ages are listed in Table 5 and Fig. 6. Uranium-series analyses of two dentine-tissue samples, ESR 4A and ESR 9A, respectively, from layers 7 and 6, were needed to calculate coupled ESR/U-series results for these two teeth. For tooth ESR 4 from layer 7, the EU ESR date is 39 ± 4 ka, while its dentine had a much later closed-system U-series date of 22.9 ± 0.1 ka. These results indicate that the dentine had gradually accumulated its uranium in nearly linear fashion. The coupled ESR/U-series age of tooth ESR 4 is $51 (+7, -9)$, and its p-value is 0.12 ± 0.31 , confirming a nearly linear uptake (for LU, $p = 0$).

For tooth ESR 9 from layer 6, the date from the ESR EU model is 38 ± 5 ka, while its dentine has a closed-system U-series date of 34.8 ± 0.4 ka; the close match indicates early uptake. The coupled ESR/U-series date for this tooth is 43

Table 2
In situ dosimetry field locations and measurements at Pech-de-l'Azé I

Designation	Layer	Square	X (m)	Y (m)	Z* (m)	Gamma spectrometer dose rate ($\mu\text{Gy/a}$)**	Corresponding teeth
GR GAM 2	7 middle	H7	1008.708	1093.069	-1.9	192	ESR 0, 1, 2, 3, 4, 5, 7,
GAM 5	7 base	H8	1008.714	1092.831	-3.081	217	18, 19, 20, 21
GAM 4	7 base	H8	1008.982	1092.444	-3.148	214	
Layer 7 Mean						208 ^o	
GAM 8	6	H8	1008.909	1092.21	-3.613	261	ESR 8, 9
GAM 1	6	H8	1008.794	1092.458	-3.627	292	
Layer 6 Mean						277 ^o	
GAM 3	5	I10	1009.788	1090.001	-3.893	215	ESR 10, 12, 13
GR GAM 1	5	I9	1008.909	1092.21	-3.613	292	
GAM 2	5	I9	1009.262	1091.693	-4.219	336	
Layer 5 Mean						281 ^o	

* Elevation (Z) in meters below datum.

** MicroGrays per year.

^o Average of gamma measurements for each layer, which was used in the age calculations for corresponding teeth; an uncertainty of $\pm 20\%$ was used on this value in the age calculations to incorporate (1) unknown variations in moisture history and (2) unknown variation in dose rate among in situ sample locations due to potential heterogeneity of the actual gamma-dose rate near teeth.

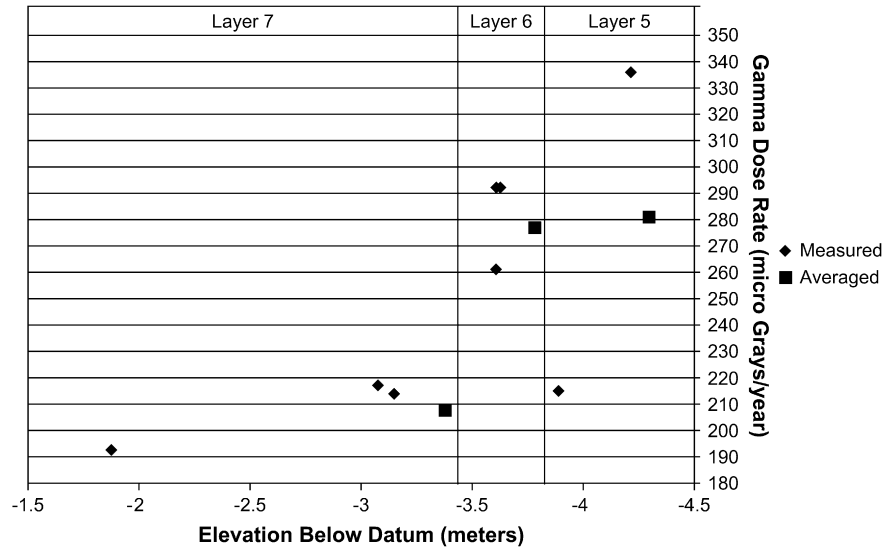


Fig. 5. A plot of gamma-dose rates versus depth in the profile. The variability in gamma-dose rate in a given archaeological layer clearly increases with its depth interval. The greatest dispersion of measured gamma-dose rates is seen in layer 5.

(+8, –6) ka, and its p-value is -0.8 ± 0.18 , confirming relatively early uptake of U (for EU, $p = -1.0$).

The coupled-ESR/U-series-age estimates are considered the best ESR-based ages for each of these layers, but we also note that they are concordant in each case with the

mean model ages (EU and LU) for each of these layers. The mean ESR-model ages (EU and LU) reported here fall within OIS 3 according to the orbitally tuned oxygen-isotope chronology established by Martinson et al. (1987) (Fig. 6).

Table 3
Analytical data for ESR dating at Pech-de-l’Azé I

Mac field #	Z (m below datum)	γ -dose rate	Sed β -dose rate	EU En α -dose rate	EU En β -dose rate	EU Den β -dose rate	EU total dose rate*	LU En α -dose rate	LU En β -dose rate	LU Den β -dose rate	LU total dose rate
<i>Layer 7</i>											
ESR 0A	-2.206	208	110	39	11	69	507	17	5	33	447
ESR 1A	-3.046	208	97	0	0	66	441	0	0	31	406
ESR18A	-3.148	208	97	0	0	71	446	0	0	34	408
ESR19A	-3.148	208	95	0	0	86	459	0	0	41	414
ESR20A	-3.148	208	84	75	23	95	555	35	11	46	454
ESR21A	-3.148	208	87	0	0	74	439	0	0	36	401
ESR21B	-3.148	208	84	0	0	87	449	0	0	41	403
ESR 2A	-3.256	208	107	94	27	62	568	43	12	30	471
ESR 3A	-3.266	208	71	36	11	157	553	17	5	76	447
ESR 3B	-3.266	208	62	0	0	172	512	0	0	83	423
ESR 4A	-3.296	208	105	0	0	186	569	0	0	90	473
ESR 5A	-3.296	208	100	70	18	160	ψ 651	33	9	78	510
ESR 5B	-3.296	208	105	0	0	143	526	0	0	69	452
ESR 7A	-3.456	208	91	78	24	111	582	36	12	54	471
<i>Layer 6</i>											
ESR 8A	-3.646	277	4	0	0	57	ψ 543	0	0	28	442
ESR 8B	-3.646	277	56	45	13	33	ψ 536	20	6	16	463
ESR 9A	-3.796	277	107	15	4	118	591	7	2	51	525
<i>Layer 5</i>											
ESR10A	-4.086	281	82	0	0	18	451	0	0	9	438
ESR12A	-4.236	281	76	0	0	35	462	0	0	17	440
ESR13A	-4.396	281	108	0	0	45	504	0	0	21	476

Notes: α = alpha; β = beta; γ = gamma; En = enamel; Den = dentine; Sed = sediment; units for all columns are $\mu\text{Gy/a}$; ψ = includes a contribution from cementum that is not listed in this table.

* Total dose rates include the cosmic doses calculated according to sample depth and overburden equal to $70 \mu\text{Gy/a}$ (microGrays per year).

Table 4
Analytical U-series data for Pech-de-l'Azé I

Dentine sample ^c	²³⁸ U concentration ppm ($\pm 2\sigma$ error)	²³⁰ Th/ ²³⁴ U*	²³⁴ U/ ²³⁸ U*	²³⁰ Th/ ²³² Th*	²³⁰ Th/ ²³⁴ U closed-system age (ka) ($\pm 2\sigma$ error)
ESR 4A	14.43 \pm 0.0206	0.1900 \pm 0.0009	1.0386 \pm 0.0031	1068 \pm 5	22.9 \pm 0.1
ESR 9A	8.92 \pm 0.0119	0.2756 \pm 0.0028	1.1067 \pm 0.0026	204 \pm 2	34.8 \pm 0.4

^c Th/U analyses were performed on dentine tissues adjacent to ESR-dated enamel by MC-ICP-MS at GEOTOP Laboratory, University of Quebec at Montreal.

* Activity ratios.

AMS ¹⁴C results

A conventional ¹⁴C age was obtained in the early 1970s by W. Mook on two kilograms of burnt bone collected in layer 4. The age was 42.23 \pm 1.34 ka (GrN 6784) (D. de Sonneville-Bordes archives). This conventional ¹⁴C age is certainly a minimum for layer 4, as it was done on several kilograms of burnt bone and before the use of ultrafiltration techniques (Bronk et al., 2004).

Table 5
ESR and U-series dating results for teeth from Pech-de-l'Azé I

Mac field #	EU ESR age (ka)*	LU ESR age (ka)*	Coupled ESR/ ²³⁰ Th / ²³⁴ U age [‡] (ka)	p-value
<i>Layer 7</i>				
ESR 0A	48 \pm 5	55 \pm 6		
ESR 1A	44 \pm 6	47 \pm 7		
ESR 18A	57 \pm 8	62 \pm 8		
ESR 19A	54 \pm 12	60 \pm 13		
ESR 20A	37 \pm 4	46 \pm 6		
ESR 21A	45 \pm 6	50 \pm 7		
ESR 21B	47 \pm 6	52 \pm 7		
ESR 2A	33 \pm 4	40 \pm 6		
ESR 3A	40 \pm 4	49 \pm 5		
ESR 3B	43 \pm 5	52 \pm 6		
ESR 4A	39 \pm 4	47 \pm 6	51 ⁺⁷ / ₋₉	0.12 \pm 0.31
ESR 5A	29 \pm 3	38 \pm 4		
ESR 5B	41 \pm 7	48 \pm 9		
ESR 7A	32 \pm 3	39 \pm 4		
Layer 7** mean	42 \pm 8	49 \pm 7		
<i>Layer 6</i>				
ESR 8A	42 \pm 5	52 \pm 7		
ESR 8B	40 \pm 5	47 \pm 6		
ESR 9A	38 \pm 5	43 \pm 6	43 ⁺⁸ / ₋₆	-0.8 \pm 0.18
Layer 6** mean	40 \pm 2	47 \pm 5		
<i>Layer 5</i>				
ESR 10A	46 \pm 7	47 \pm 7		
ESR 12A	44 \pm 6	45 \pm 6		
ESR 13A	57 \pm 8	60 \pm 8		
Layer 5** mean	49 \pm 6	51 \pm 7		

All ages were calculated assuming 10 \pm 10% moisture.

* Errors reported for EU and LU ESR ages are $\pm 1\sigma$.

** Mean age for each layer reported with $\pm 1\sigma$ values (population standard deviation of the mean).

‡ Coupled ESR/²³⁰Th/²³⁴U ages (referred to as ESR/U-series ages in the text) were calculated assuming a concentration of 0.01 ppm uranium in the enamel (actual values of U in the enamels were measured by delayed neutron counting to be less than 0.1 ppm). These ages were also calculated assuming ²³⁴U/²³⁸U and ²³⁰Th/²³⁴U activity ratios for the enamel to be the same as that found in the dentine of the same tooth.

We recently obtained two AMS ¹⁴C ages for the top of layer 6 from two unburnt specimens of cortical bone. These ages were reported by J. van der Plicht from Centrum voor Isotopen Onderzoek in Groningen and are listed in Table 6.

There is no consensus on the radiocarbon calibration for ages prior to 26 ka. According to the Fairbanks0805 calibration (Fairbanks et al., 2005), the calendar ages would be 42.9 \pm 0.5 ka cal BP and 42.0 \pm 0.3 ka cal BP. Applying the CalPal2005_SFCP calibration (Weninger et al., 2005), the calendar ages would be 43.1 \pm 0.5 ka cal BP and 42.2 \pm 0.3 ka cal BP. Using the extreme values of both calendar-age conversions, the overall age lies between 41.7 and 43.6 ka cal BP.

Summary of geochronology

Table 7 provides a comparison among the dating results obtained in this study (layers 5, 6, and 7), along with an earlier unpublished ¹⁴C-age determination by Mook in the late 1970s for layer 4. The italicized results provide the best estimates of burial ages for teeth in each of the three layers dated with ESR.

The low concentration of uranium in the teeth from layer 5 allow us to use the age of the mean EU and LU ages (plus/minus their one-sigma errors) to constrain its age between 43 and 58 ka. Layer 6 is dated by both AMS ¹⁴C and a coupled-ESR/U-series-age estimate. The calibrated ¹⁴C estimates yield a range of 41.7 to 43.6 ka cal BP, which agrees well with the coupled ESR/U-series age of 43 (+8, -6) ka on tooth ESR 9.

The uppermost layer, layer 7, only has ESR-model ages and a coupled ESR/U-series age on tooth ESR 4 of 51 (+7, -9) ka. This age yields a range of 42 to 58 ka, which is concordant with the mean EU ESR age of 42 \pm 8 ka (68% confidence) and the mean LU ESR age of 49 \pm 7 ka (68% confidence).

Finally, where we did not have two independent methods of dating available, we used the principle of superposition to constrain the ages of the uppermost and lowermost units at the site. The age of the lowermost layer, layer 4, is constrained to be greater than 43 ka (34% confidence level) by the overlying layer 5's minimum mean EU ESR age. This agrees well with the uncalibrated ¹⁴C age on burnt bone of 42.23 \pm 1.34 ka BP from layer 4 itself, which is considered a minimum age. The uppermost layer, layer 7, must be younger than 43.6 ka cal BP when using ¹⁴C as the constraining age in the underlying unit, and it must be younger than 51 ka when using coupled ESR/U-series.

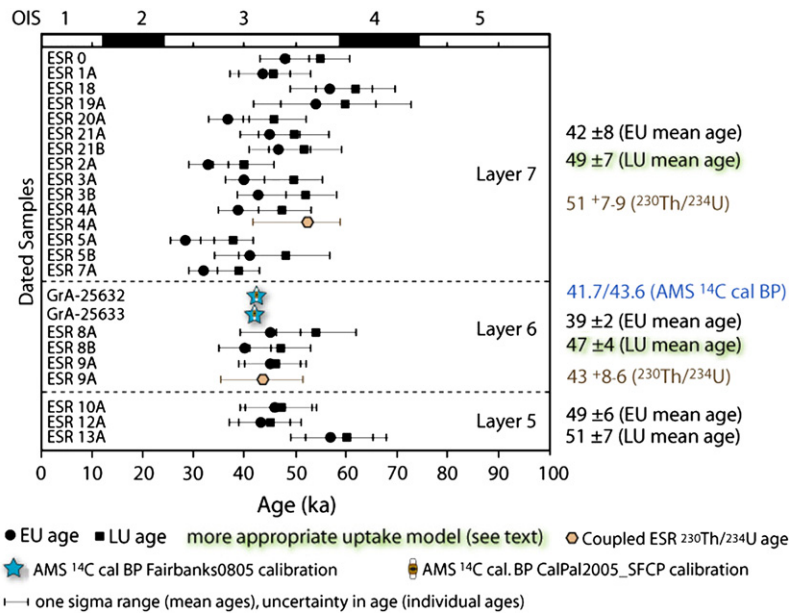


Fig. 6. Diagram of radiometric ages obtained for Pech-de-l'Azé I layers 5–7 (OIS boundaries after Martinson et al., 1987).

Comparison with other southwestern France MTA (B) sites

There are only three sites at which MTA (B) layers have been dated by absolute dating methods: Barbas III, La Rochette, and Le Moustier. The MTA (B) layer at Barbas III (C.4) was dated by ^{14}C to 38.3 ± 5 ka BP and 43.5 ± 2.2 ka BP (Boëda et al., 1996), which would correspond to about 42.8 ± 0.4 and 47.0 ± 0.2 ka cal BP, respectively, according to Fairbanks et al. (2005) and to 42.4 ± 5 and 47.1 ± 2.0 ka cal BP, respectively, according to the CalPal2005_SFCP curve (Weninger et al., 2005). La Rochette's layer 7 was recently dated to 42.6 ± 1.6 ka and 52.5 ± 3.4 ka by the AMS radiocarbon method (Valladas, unpublished in Soressi, 2002: 36–37); the first age would correspond to 46.3 ± 1.6 ka cal BP age according to the CalPal2005_SFCP curve (Weninger et al., 2005) [Fairbanks et al. (2005) did not provide a conversion for a radiocarbon age equal to 42.6 ± 1.6 ka, and there are no available calibration curves for radiocarbon ages older than 50 ka]. Le Moustier's layer H was dated by TL and ESR methods, producing results that are quite consistent with one another. Twenty-four burnt flints yielded average ages of 42.5 ± 2 ka and 46.3 ± 3 ka for layers H2–H9 and layer H1, respectively, for an overall averaged age of 44 ka (Valladas et al., 1986; Mercier et al., 1995). The mean ESR EU and LU ages ($n = 19$) for the MTA (B) industry are 39.7 ± 2.4 ka and 41 ± 2.6 ka, respectively (Mellars and Grün, 1991). The absolute ages of the MTA (B) from these three sites, as well as the ones from Pech-de-l'Azé I, fall within OIS 3.

Our results agree well with the ages of MTA (B) at these other sites. The MTA (B) of layer 5 is dated to 43–58 ka when using the combined mean ESR EU and LU age range. The MTA (B) of layer 6 is dated by AMS ^{14}C to about 41.7–43.6 cal BP and by coupled ESR/U-series to 37–51 ka. The MTA (B) of layer 7 is dated to 41–58 ka by coupled ESR U-series, but to less than 51 ka by superposition above layer 6 (see Table 7 footnotes).

Conclusions

Our analysis of the unpublished archives of Peyrony, Bordes, and others shows that the Pech-de-l'Azé I Neandertal child was discovered at the bottom of layer 6, attributed to the MTA type B. Consequently, this fossil child cannot be older than the formation of layer 6 and cannot be younger than the formation of layer 7, which closes the sequence at Pech-de-l'Azé I and is also attributed to the MTA type B. These skull and mandible are the first diagnostic human remains (aside from an isolated tooth) recovered in a MTA type B context. Consequently, Neandertals must be considered the makers of this Mousterian industry, which shows an unusual high frequency of Upper Paleolithic type tools, elongated blanks, and blades (Bordes, 1984: 142–149; Soressi, 2002: 218–238). Based on coupled ESR/U-series ages, the Neandertal child cannot be older than 51 ka or younger than 41 ka. This estimate is consistent with the calibrated AMS ^{14}C dates of about 41.7–43.6 ka cal BP, calibrated using the Fairbanks0805 (Fairbanks et al., 2005) or the CalPal2005_SFCP

Table 6
AMS ^{14}C ages obtained for the base of layer 7 and the top of layer 6 (the 3D coordinates of each sample at the site are also indicated)

Groningen ref.	Bone square-ID	Layer	X (m)	Y (m)	Z (m)	Age (years BP)
GrA-25632	PAI F10 412	6-top	1006.35	1090.64	−3.456	38430^{+560}_{-470}
GrA-25633	PAI F10 432	6-top	1006.61	1090.68	−3.476	37060^{+490}_{-420}

Table 7
Summary of geochronology at Pech-de-l'Azé I

Layer	¹⁴ C age			Coupled ESR/ U-series age (ka)	Coupled ESR/ U-series or ESR age range (ka)	Mean ESR		Superpos. age (ka cal BP, or ka)
	Uncal (ka BP)	Cal (ka cal BP)	Cal age range (ka cal BP)			EU age (ka)	LU age (ka)	
7				51 ⁺⁷ / ₋₉	41–58*	42 ± 8 (n = 14)	49 ± 7 (n = 14)	<43.6 [§] <51 ^{§§}
6	37.06 ^{+0.49} / _{-0.42} 38.43 ^{+0.56} / _{-0.47}	42.9 [†] 42.0 [‡] 43.1 [†] 42.2 [‡]	41.7–43.6	43 ⁺⁸ / ₋₆	37–51*	40 ± 2 (n = 3)	47 ± 5 (n = 3)	
5					43–58**	49 ± 6 (n = 3)	51 ± 7 (n = 3)	
4	42.23 ± 1.43 [‡]							>43 ^{§§§}

Notes: EU = early uptake; LU = linear uptake; uncertainty in mean is one sigma; Uncalib = uncalibrated; Cal = calibrated; Superpos. = principle of superposition. Italicized values are considered the best age estimates for formation of the layers obtained by ESR or coupled ESR/U-series dating.

[‡] Considered a minimum age obtained on several kg of burned bone by W. Mook in the early 1970s (GrN 6784) (D. de Sonneville-Bordes archives).

[†] Based on calibration of Fairbanks et al. (2005).

[‡] Based on calibration of Weninger et al. (2005).

* Range based on minimum and maximum value of coupled ESR/U-series age on an individual tooth and its uncertainty.

** Range based on minimum EU ESR age and maximum LU ESR age at only 34% confidence level.

[§] Obtained by comparison with calibrated ¹⁴C age in underlying layer 6.

^{§§} Obtained by comparison with coupled ESR/U-series age plus its uncertainty in underlying layer 6.

^{§§§} Obtained by comparison with mean EU ESR age minus its uncertainty in overlying layer 5.

(Weninger et al., 2005) calibrations. In addition, the ESR ages of the MTA industries at Pech-de-l'Azé I are in good agreement with estimates of the same industry from around the local region. The age of layer 4, at the base of the sequence, is constrained to >43 ka (34% confidence level) by the minimum mean ESR EU age in the overlying layer, which is in good agreement with expectation from Mook's layer 4 uncalibrated ¹⁴C age for burned bone of 42.2 ± 1.3 ka BP, which we consider to be a minimum age.

Considering the age of layers 6 and 7 at Pech-de-l'Azé I, and considering that: the MTA type B has always been recovered underneath the MTA type A (Bordes, 1984: 149; Mellars, 1996: 189), and that the same method of manufacturing stone-tools appear to have been used in both MTA type A and B (Soressi, 2004), it is safe to assume that the MTA type A was also produced by Neandertals, as was the MTA type B. As the oldest Aurignacian industry in the local region is younger than 41 ka cal BP (Mellars, 2006), the MTA type A and B from layer 4 to 6 (and may be layer 7) had been manufactured by Neandertals immediately before the arrival of modern human in this region. Yet, recent technological analyses of the MTA have shown that some behaviors previously thought to be characteristics of more recent behaviors associated with anatomically modern humans had already been developed by Neandertals, within the MTA (Soressi, 2005). Moreover, some of these specific behaviors (such as the scheduling of lithic tool production within the territory) had been probably abandoned within the MTA type B, while others (the use of a volumetric method of producing blanks) were continued. The use of a volumetric method of producing blanks and the interest for backed tools were consistently maintained by Neandertals, in the same region, from the MTA type A, through the MTA type B, till the Chatelperronian (Soressi, 2004; 2005). The contextualization and the dating of Pech-de-l'Azé

I Neandertal show indeed that the evolutionary trajectory of the last Neandertals in south-western Europe might have been punctuated by a series of behavioral changes. Additionally, the precise radiometric dating of the layer that contained the Pech-de-l'Azé I individual allows us to include it within the sample of the most recent southwestern European Neandertals. Ontogenetic variation between Pech-de-l'Azé I and other children of the same age class from the same region, such as the Roc de Marsal 1 individual, has been described (Tillier, 1996), and thus, this study is a new step toward differentiating temporal from individual variation in late Neandertals in this region. A geographical approach to the biological and cultural changes of late Pleistocene European hominids is clearly needed.

Acknowledgements

M. Soressi thanks the Ministry of Culture of France, the Conseil Général de la Dordogne, as well as the "ACR Paléolithique moyen," directed by J.-P. Texier and J. Jaubert, for contributing funding to this project. The Musée National de Préhistoire (Les Eyzies de Tayac, France) and Mme. de Sonneville-Bordes granted M. Soressi access to Bordes's collection and archives. The Musée de l'Homme (Paris, France) authorized B. Maureille to study M. Boule's unpublished archives. W.J. Rink and H.L. Jones thank the Natural Sciences and Engineering Research Council of Canada for financial support. M. Soressi thanks P. Mellars for his support at the initiation of this project. The plot of the pieces provided within this paper was made with New Plot software created by S.J.-P. McPherron and H. Dibble. In the end, none of these analyses could have taken place without the dedicated work of F. Lacrampe, L. Daulny, and others on the curation of Bordes's collection.

References

- Armand, D., Pubert, E., Soressi, M., 2001. Organisation saisonnière des comportements de prédation des Moustériens de Pech-de-l'Azé I. Premiers résultats. *Paléo* 13, 19–28.
- Boëda, E., Fontugne, M., Valladas, H., Ortega, I., 1996. Barbas III. Industries du paléolithique moyen récent et du Paléolithique supérieur ancien. In: Carbonell, E., Vaquero, M. (Eds.), *The Last Neandertals, the First Anatomically Modern Humans: A Tale about Human Diversity. Cultural Change and Human Evolution: The Crisis at 40 Ka BP*. Universitat Rovira i Virgili, Terragona, pp. 147–156.
- Bordes, F., 1953. Essai de classification des industries 'moustériennes'. *Bulletin de la Société Préhistorique Française* 50, 457–466.
- Bordes, F., 1954. Les gisements du Pech-de-l'Azé (Dordogne). *L'Anthropologie* 58, 401–432.
- Bordes, F., 1955. Les gisements du Pech-de-l'Azé (Dordogne). *L'Anthropologie* 59, 1–38.
- Bordes, F., 1961. Mousterian cultures in France. *Science* 134, 803–810.
- Bordes, F., 1972. *A Tale of Two Caves*. Harper & Row, New York.
- Bordes, F., 1975. Le gisement de Pech-de-l'Azé IV: note préliminaire. *Bull. Soc. Préhist. Fr.* 2, 293–308.
- Bordes, F., 1984. Leçons sur le Paléolithique. In: *Cahiers du Quaternaire* 7, CNRS, Paris.
- Bordes, F., Bourgon, M., 1950. Le gisement de Pech de l'Azé-Nord: prise de date et observations préliminaires. *Bull. Soc. Préhist. Fr.* 4, 381–383.
- Bordes, F., Bourgon, M., 1951. Le complexe Moustérien: moustériens, levalloisien et tayacien. *L'Anthropologie* 55, 1–23.
- Brennan, B.J., Rink, W.J., McGuirol, E.L., Schwarcz, H.P., Prestwich, W.V., 1997. Beta doses in tooth enamel by "one-group" theory and the ROSY ESR dating software. *Radiat. Meas.* 27, 307–314.
- Brennan, B.J., Rink, W.J., Rule, E.M., Schwarcz, H.P., Prestwich, W.V., 1999. The Rosy ESR dating program. *Ancient TL* 17, 45–53.
- Bronk, R.C., Higham, T., Bowles, T., Hedges, R., 2004. Improvements to the pretreatment of bone at Oxford. *Radiocarbon* 46, 155–163.
- Capitan, L., Peyrony, D., 1909. Deux squelettes humains au milieu de foyers de l'époque moustérienne. *Revue de l'Ecole d'Anthropologie*, 402–409.
- Capitan, L., Peyrony, D., 1910. Deux squelettes humains au milieu des foyers de l'époque moustérienne. *Bull. Mém. Soc. Anthropol. Paris* 1-IV, 48–53.
- Debénath, A., Jelinek, A.J., 1998. Nouvelles fouilles à La Quina (Charente). Résultats préliminaires. *Gallia Préhistoire* 40, 29–74.
- Fairbanks, R.G., Mortlock, R.A., Chiu, T., Cao, L., Kaplan, A., Guilderson, T.P., Fairbanks, T.W., Bloom, A.L., 2005. Marine radiocarbon calibration curve spanning 0 to 50,000 years B.P. based on paired $^{230}\text{Th}/^{234}\text{U}/^{238}\text{U}$ and ^{14}C dates on pristine corals. *Quatern. Sci. Rev.* 24, 1781–1796.
- Ferembach, D., 1969. Les affinités morphologiques de l'enfant néandertalien du Pech-de-l'Azé (Dordogne). *Comptes rendus de l'Académie des Sciences de Paris* 268-D, 1485–1488.
- Ferembach, D., Legoux, P., Fenart, R., Empereur-Buisson, R., Vlcek, E., 1970. L'enfant du Pech-de-l'Azé. In: *Arch. Inst. Paléontol. Humaine*, 33. Masson & Cie, Paris.
- Grün, R., Schwarcz, H.P., Chadam, J.M., 1988. ESR dating of tooth enamel: coupled corrections for U-uptake and U-series disequilibrium. *Nucl. Tracks Radiat. Meas.* 14, 237–241.
- Grün, R., McDermott, F., 1994. Open system modeling for U-series and ESR dating of teeth. *Quatern. Sci. Rev.* 13, 121–125.
- Hublin, J.-J., 1988. Les presapiens Européens. In: Trinkaus, E. (Ed.), *L'Homme de Néandertal*, vol. 3: l'Anatomie. *Eraul* 30, Liège, pp. 75–80.
- Jones, H.L., Rink, W.J., Schepartz, L.A., Miller-Antonio, S., Huang, W., Ellwood, B.B., 2004. Coupled electron spin resonance (ESR)/uranium-series dating of mammalian tooth enamel at Panxian Dadong, Guizhou Province, China. *J. Archaeol. Sci.* 31, 975–977.
- Marsh, R.E., Prestwich, W.V., Rink, W.J., Brennan, B.J., 2002. Monte Carlo determinations of the beta dose rate to tooth enamel. *Radiat. Meas.* 35, 609–616.
- Martinson, D.G., Piasias, N.G., Hays, J.D., Imbrie, J., Moore Jr., T.C., Shackleton, N.J., 1987. Age dating and the orbital theory of the ice ages: development of a high-resolution 0 to 300,000-year chronostratigraphy. *Quatern. Res.* 27, 1–29.
- Maureille, B., Soressi, M., 2000. Sur la position chronostratigraphique du crâne humain du Pech-de-l'Azé (commune de Carsac, Dordogne): la ré-urrection du fantôme. *Paléo* 12, 339–352.
- McPherron, S., Dibble, H.L., 2000. The lithic assemblages of Pech de l'Azé IV (Dordogne, France). *Préhistoire Européenne* 15, 9–20.
- Mellars, P., 1996. *The Neanderthal Legacy. An Archaeological Perspective from Western Europe*. Princeton University Press, Princeton.
- Mellars, P., 2006. Archeology and the dispersal of modern humans in Europe: deconstructing the "Aurignacian". *Evol. Anthropol.* 15, 167–182.
- Mellars, P., Grün, R., 1991. A comparison of the electron spin resonance and thermoluminescence dating methods: the results of ESR dating at Le Moustier (France). *Cambridge Archaeol. J.* 1, 269–276.
- Mercier, N., Valladas, H., Valladas, G., 1995. Flint thermoluminescence dates from the CFR Laboratory at GIF: contributions to the study of the chronology of the Middle Palaeolithic. *Quatern. Sci. Rev.* 14, 351–364.
- Orlando, L., Darlu, P., Toussaint, M., Bonjean, D., Otte, M., Hänni, C., 2006. Revisiting Neandertal diversity with a 100,000 year old mtDNA sequence. *Curr. Biol.* 16, 400–402.
- Patte, E., 1957. L'enfant Néandertalien du Pech-de-l'Azé. Masson & Cie, Paris.
- Peyrony, D., 1920. Le Moustérien—ses faciès. Association Française pour l'avancement des Sciences, 44^e session, Strasbourg, pp. 1–2.
- Rink, W.J., 1997. Electron spin resonance (ESR) dating and ESR applications in Quaternary science and archaeometry. *Radiat. Meas.* 27, 975–1025.
- Rink, W.J., 2000. Beyond ^{14}C dating: A user's guide to long range dating methods in archaeology. In: Goldberg, P., Holliday, V.T., Ferring, C.R. (Eds.), *Earth Sciences and Archaeology*. Kluwer Academic/Plenum Press, pp. 385–417.
- Schwarcz, H.P., 1985. ESR studies of tooth enamel. *Nucl. Tracks Radiat. Meas.* 10, 865–867.
- Schwarcz, H.P., 1994. Current challenges to ESR dating. *Quatern. Sci. Rev.* 13, 601–605.
- Schwarcz, H.P., Blackwell, B., 1983. $^{230}\text{Th}/^{234}\text{U}$ age of a Mousterian site in France. *Nature* 301, 236–237.
- Soressi, M., 2002. Le Moustérien de tradition acheuléenne du sud-ouest de la France. Discussion sur la signification du faciès à partir de l'étude comparative de quatre sites: Pech-de-l'Azé I, Le Moustier, La Rochette et la Grotte XVI. Thèse de l'Université Bordeaux I. Available online at <www.paleosoc.org>.
- Soressi, M., 2004. From Mousterian of acheulian tradition type A to type B: technical tradition, raw material, task, or settlement dynamic changes? In: Conard, N.J. (Ed.), *Settlement Dynamics of the Middle Paleolithic and Middle Stone Age*, vol. 2. Tübingen Publications in Prehistory, pp. 343–366.
- Soressi, M., 2005. Late Mousterian lithic technology. Its implications for the pace of the emergence of behavioural modernity and the relationship between behavioural modernity and biological modernity. In: Backwell, L., d'Errico, F. (Eds.), *From Tools to Symbols*. University of Witwatersand Press, pp. 389–417.
- Soressi, M., Armand, D., d'Errico, F., Jones, H.L., Pubert, E., Rink, W.J., Texier, J.-P., Vivent, D., 2002. Pech-de-l'Azé I (Carsac, Dordogne): nouveaux travaux de recherche sur le Moustérien de tradition acheuléenne. *Bull. Soc. Préhist. Fr.* 99, 5–11.
- Tillier, A.-M., 1996. The Pech-de-l'Azé and Roc de Marsal children (Middle Paleolithic, France): skeletal evidence for variation in Neanderthal ontogeny. *Hum. Evol.* 11, 113–119.
- Valladas, H., Geneste, J.-M., Joron, J.-L., Chadelle, J.-P., 1986. Thermoluminescence dating of Le Moustier (Dordogne, France). *Nature* 322, 452–454.
- Vallois, H.-V., 1958. La grotte de Fontéchevade. Deuxième partie: *Anthropologie*. *Arch. Inst. Paleontol. Hum.* 29, 1–64.
- Vaufrey, R., 1933. Le Moustérien de tradition acheuléenne au Pech de l'Azé (Dordogne). *L'Anthropologie* 43, 425–427.
- Verna, Ch., 2006. Les restes humains moustériens de la Station Amont de La Quina – (Charente, France). Thèse de l'Université Bordeaux I.
- Weninger, B., Jöris, O., Danzeglocke, U., 2005. Cologne Radiocarbon CALibration & PALaeoclimate Research Package: CalPal_2005_SFCP Calibration Curve. Available online at <www.calpal.de>.